HHS Public Access

Author manuscript

J Neurosci Res. Author manuscript; available in PMC 2015 April 28.

Published in final edited form as:

J Neurosci Res. 2014 October ; 92(10): 1319–1329. doi:10.1002/jnr.23413.

Reductions of the components of the calreticulin/calnexin quality-control system by proteasome inhibitors and their relevance in a rodent model of Parkinson's disease

Xiu-Li Kuang[1,2], **Fang Liu**[1,2], **Huifang Chen**[1,2], **Yiping Li**[3], **Yimei Liu**[1,2], **Jian Xiao**[1,2], **Ge Shan**[4], **Mingjie Li**[5], **B. Joy Snider**[5], **Jia Qu**[1,2], **Steven W. Barger**[6,7], and **Shengzhou Wu**[1,2,*]

[1]School of Optometry and Ophthalmology and Eye Hospital, Wenzhou Medical University, Wenzhou, Zhejiang, People's Republic of China

[2]State Key Laboratory Cultivation Base and Key Laboratory of Vision Science, Ministry of Health, Zhejiang Provincial Key Laboratory of Ophthalmology and Optometry, Wenzhou, Zhejiang, People's Republic of China

[3]Laboratory of Molecular Cell Biology, Institute of Biochemistry and Cell Biology, Shanghai Institutes for Biological Sciences, Chinese Academy of Sciences, Shanghai, People's Republic of China

[4]School of Life Sciences and CAS Key Laboratory of Brain Function and Disease, University of Science and Technology of China, Hefei, Anhui Province, People's Republic of China

[5]Department of Neurology, Washington University School of Medicine, St. Louis, Missouri

[6]Department of Geriatrics, University of Arkansas for Medical Sciences, Little Rock, Arkansas

[7]Geriatric Research Education and Clinical Center, Central Arkansas Veterans Healthcare System, Little Rock, Arkansas

Abstract

Evidence indicates that the ubiquitin-proteasome system and the endoplasmic retculum (ER) quality-control system work in concert to ensure that proteins are correctly folded in the ER and that misfolded proteins are retrotransported to the cytosol for degradation by proteasomes. Dysfunction of either system results in developmental abnormalities and even death in animals. This study investigates whether and how proteasome inhibition impacts the components of the calreticulin (CRT)/calnexin (CNX) glycoprotein folding machinery, a typical ER protein quality-control system, in the context of early neuronal injury. Here we report that proteasome inhibitor treatments, at nonlethal levels, reduced protein levels of CRT and ERp57 but not of CNX. These treatments increased protein levels of CRT in culture media, an effect blocked by brefeldin A, an inhibitor of protein trafficking; by contrast, ERp57 was not detected in culture media. Knockdown of CRT levels alone increased the vulnerability of SH-SY5Y, a neuronal cell line, to 6-hydroxydopamine (6-OHDA) toxicity. In a rat model of Parkinson's disease, intrastriatal 6-OHDA

*Correspondence to: Dr. Shengzhou Wu., MD, PhD, Key Laboratory of Visual Science, National Ministry of Health, School of Optometry and Ophthalmology, Wenzhou Medical University, Zhejiang Province, People's Republic of China 325027, wszlab@mail.eye.ac.cnorshzhwu1@gmail.com.

lesions resulted in decreased levels of CRT and ERp57 in the midbrain. These findings suggest that reduction of the components of CRT/CNX glycoprotein quality-control system may play a role in neuronal injury in Parkinson's disease and other neurodegenerative disorders associated with dysfunction of the ubiquitin-proteasome system.

INTRODUCTION

The ubiquitin-proteasome system (UPS) is one of the major intracellular protein degradation systems, regulating a broad range of processes including the cell cycle, apoptosis, and cell signaling (Hochstrasser, 1995; Koepp et al., 1999). Inhibition of the UPS may play a role in Alzheimer's disease (AD), Parkinson's disease (PD), and amyotrophic lateral sclerosis (ALS; Keller et al., 2000a; McNaught, 2004; Deng et al., 2011; Tashiro et al., 2012). Reports have shown that proteasome activity is decreased in the substantia nigra in PD (McNaught and Jenner, 2001; McNaught et al., 2003) and in affected brain regions in AD (Keller et al., 2000a). Conditional knockout of a proteasome subunit reproduces aspects of ALS in mice (Tashiro et al., 2012).

Endoplasmic reticulum (ER) is responsible for many important functions, including protein synthesis, posttranslational modifications, protein quality control, calcium storage, and intracellular signaling. ER employs two mechanisms to cope with misfolded proteins. The first is a program of responses termed the unfolded protein response (UPR), which is used to adjust to ER stresses via transcriptional or translational regulation; the second is ER-associated degradation (ERAD), which recognizes terminally misfolded proteins and retrogradely transports them to cytosol, where they are degraded by the UPS (Bukau et al., 2006). During these processes of quality surveillance, the calreticulin (CRT)/calnexin (CNX) lectin chaperone system participates in structural maturation and determines the destiny of some proteins (Ellgaard and Frickel, 2003). The interaction involves the concerted activities of the lectin chaperones CRT, an ER lumenal protein; CNX, an ER membrane-integral protein; and their cochaperone, ERp57. In concert with ERp57, either CRT or CNX associates with newly synthesized, monoglucosylated proteins in ER to tag slightly or intermediately misfolded glycoproteins with an extra glucose subunit; this causes their retention in the ER for refolding.

These proper functions of CRT/CNX are demonstrated by the debilitating phenotypes that result from genetic ablation of either CRT or CNX in mice (Mesaeli et al., 1999; Rauch et al., 2000; Denzel et al., 2002). In addition to participating in quality control in the ER, CRT plays roles in a wide range of processes, including calcium buffering (Gelebart et al., 2005), gene regulation (Burns et al., 1994), cell adhesion (Fadel et al., 1999), and wound healing (Greives et al., 2012). Regulation of CRT is versatile; expression and activity of CRT can be changed by different kinds of cell stressors, including chemotherapeutic drugs, internal-store calcium manipulation, heat shock protein, and heavy metals (Nguyen et al., 1996; Waser et al., 1997; Tufi et al., 2008); ER calcium depletion increases the secretion and membrane expression of CRT (Peters and Raghavan, 2011).

Some studies indicate that proteasome inhibition can lead to ER stress. Proteasome inhibition increases transcription of ER stress marker proteins, including GRP78/BiP and

GRP94 (Bush et al., 1997). Proteasome inhibition results in phosphorylation of eIF2α via activation of general control nonderepressible 2 (GCN2) in mouse embryonic fibroblasts, leading to reductions in protein synthesis (Jiang and Wek, 2005). We have found that proteasome inhibition can deplete ER calcium stores in primary mouse neurons (Wu et al., 2009); depletion of ER calcium is one type of ER stress (Paschen, 2003; Peters and Raghavan, 2011). Considering that proteasome inhibition usually induces protein aggregation, which may impact the ER protein quality-control system, we examined whether and how proteasome inhibition changes the CRT/CNX glycoprotein quality-control system and underlying mechanisms. We further examined the impact on cell survival by lowering one component of the CRT/CNX system. Finally, we examined the functional consequences in a rat model of PD.

MATERIALS AND METHODS

Materials

The following substances, materials, and reagents (and suppliers) were used in this study: 3,3′,5,5′-tetramethylbenzidine (TMB), carbobenzoxy-L-leucyl-L-leucyl-L-leucinal, clasto-lactacystine-β-lactone, adenosine triphosphate, DL-dithiothreitol, ethylene glycol tetraacetic acid (EGTA), ethylenediaminetetraacetic acid (EDTA), digitonin, glycerine, N-succinyl-Leu-Leu-Val-Tyr-7-amido-4-methylcoumain, 6-hydroxydopamine, apomorphine, 7-amino-4-methylcoumarin, 3,3′-diaminobenzidine, and microsome isolation kits (Sigma, St. Louis, MO); biotinylated anti-mouse secondary antibody and 3-amino-9 ethylcarbazole (AEC; Vector Laboratories, Burlingame, CA); tyrosine hydroxylase antibody (EMD-Millipore, Billerica, MA); CRT, HSP60, ERp57, and GAPDH antibodies (Cell Signaling Technology, Danvers, MA); purified mouse BiP/GRP78 and calnexin antibodies (BD Biosciences, San Jose, CA); LI-COR IRDye 800CW secondary antibody (LI-COR, Lincoln, NE); neutral balsam (Shanghai Pharmacy Company, Shanghai, China); fura-2/AM, mag-fura-2/AM, and Neurobasal/B27 (Molecular Probes/Invitrogen, Carlsbad, CA); full-range rainbow molecular-weight markers (GE Healthcare, Piscataway, NJ); CL-XPosure film (Thermo Scientific Branch, Shanghai, China); Pierce ECL Western Blotting Substrate (Thermo Scientific, Rockford, IL); protease inhibitor cocktail (Calbiochem, San Diego, CA); Celltiter 96 aqueous nonradioactive cell-proliferation assay kits (Promega, Madison, WI); and the CRT shRNA lentivirus transfer plasmid carrying GFP fluorescence (Origene, Rockville, MD).

Animals

Sprague-Dawley rats were purchased from the Shanghai Animal Experimental Center, Chinese Academy of Sciences, and housed in standard animal facilities with automatic illumination on a 12-hr cycle at Wenzhou Medical University. All experimental procedures adhered to the NIH Guide for the care and use of laboratory animals and the principles presented in the “Guidelines for the use of animals in neuroscience research” by the Society for Neuroscience. All procedures including minimizing the number of animals used and animal discomfort were approved by the Animal Use and Care Committee of Wenzhou Medical University.

Primary Cortical Neuronal Cultures

Primary cultures of neocortical neurons were established from E18 Sprague-Dawley rats as described previously (Li et al., 2001). Cultures were maintained in Neurobasal/B27 for 8–10 days before use in experiments. The subsequent steps in culture procedures were very similar to the primary cultures of cortical neurons described previously (Wu et al., 2004).

Western Blot and Dot Blot Analysis

Cell culture medium was collected and frozen for the sandwich ELISA experiments (below). Cells were washed once with PBS and lysed by addition of Super RIPA buffer containing a protease-inhibitor cocktail (Sigma). With regard to the blottings for rat brains, the brain samples were homogenized and then sonicated in RIPA buffer containing protease-inhibitor cocktail and centrifuged at 13,000 rpm for 10 min at 4°C. The supernatants were then collected for immunoblotting. During the blotting procedure, the nitrocellulose membranes carrying the transferred proteins from SDS-PAGE were incubated with individual primary antibody CRT (1:250)/GRP78 (1:1,000)/CNX (1:1,000)/ERp57 (1:500) overnight at 4°C, and followed by incubating with an infrared fluorescent dye-labeled secondary antibody, LI-COR IRDye 800CW (1:5,000), at room temperature for 1 hr. The images were acquired with LI-COR Odyssey imager 9120, and the band optical densities were obtained in ImageJ. GAPDH blotting (1:1,000) was used as internal loading reference. For quantification of CRT or ERp57 from microsome, a general dot blot protocol was used; proteins were deposited directly onto nitrocellular membranes, and the subsequent procedures were similar to Western blot development (Jiang et al., 2011).

ER Isolation

ER isolation was performed with a microsome-preparation kit (Sigma) according to the product manual. Briefly, cultured neurons were detached and suspended in hypotonic extraction buffer to allow cells to swell. The pellets after centrifugation were suspended in isotonic buffer, and the cells were broken with a homogenizer. The homogenates were centrifuged at 1,000g for 10 min at 4°C, and the thin floating lipid layer and pellets were discarded. The supernants were collected and subjected to centrifugation at 12,000g for 15 min at 4°C. The supernants were collected after removal of the second surface-floating lipid layer and precipitated with calcium chloride, followed by a medium-speed centrifugation (8,000g) to obtain rough-ER-enriched microsomes. The protease-inhibitor cocktail was added to hypotonic and isotonic buffers before use. Western blots against calnexin (positive) and hsp60 (negative; not shown) were used to confirm the purity of ER isolation.

Examination of CRT Secretion by Sandwich ELISA

As described above, cortices and substantia nigra (SN) of E18 rat embryos were used for neuronal culture. Liver tissues were used for extracting total proteins as standards for CRT, because there is abundant ER in liver tissues. Briefly, suitable amounts of liver were harvested from the euthanized rats, the fat tissues on the surface were removed, and the rest was washed with PBS to remove residual blood. Then, the tissue was cut into pieces and homogenized by sonication in Super RIPA protein lysis buffer containing protease-inhibitor cocktail. The homogenates were centrifuged at 13,000g at 4°C for 10 min to remove

insoluable pellets. The protein concentrations were quantified with a BCA reaction (Beyotime, Beijing, China), and a series of protein concentrations was used as standards for the subsequent ELISA. A CRT capture antibody (1:1,000; Cell Signaling) was first diluted in 0.1 M bicarbonate buffer, pH 9.2, and then 50 μl was added to each well of the microtiter plates. The antibody-coated plates were covered with paraffin film in a moist box containing a wet paper towel and incubated at 4°C overnight. The remaining buffer was removed, and the unoccupied sites were blocked with 100 μl blocking buffer containing 100 mM phosphate buffer, pH 7.2, 1% BSA, and 0.5% Tween-20 for 1 hr at room temperature, followed by washing with buffer (100 mM phosphate buffer, 150 mM NaCl, 0.2% BSA, and 0.05% Tween-20). Then, the samples and standard solutions were diluted in antigen buffer (100 mM phosphate buffer, 150 mM NaCl) and added to the antibody-coated plates in a volume of 50 μl per well. The plates were incubated at room temperature for 45–60 min, followed by washing with buffer. CRT antibody (1:500) was diluted as described above and added to the plates, followed by incubating at 4°C overnight. Horseradish peroxidase (HRP)-labeled secondary antibody (1:2,000; Beyotime) was diluted in 0.1 M bicarbonate buffer, pH 9.2, and then 50 μl was added to each well and incubated at room temperature for 30 min. TMB was used to indicate the reaction, and 1 N H2SO4 was used to stop the reaction when a deep yellow color developed. The intensities of absorption were measured with spectrophotometry (Spectra M5; Molecular Devices, Sunnyvale, CA) at 450 nM.

Establishment of Stable CRT Knockdown SH-SY5Y

SH-SY5Y (<20 passages) were transfected with plasmids carrying gene fragments expressing CRT shRNA, EGFP, and puromycin selection marker (Origene) with the help of Lipofectamine 2000 (Invitrogen). Four shRNA (H1–H4) were individually transfected or in combination into SH-SY5Y and further selected with puromycin (6 μg/ml) and the purified colonies were then multiplied. As a result of screening, the combination of H1 and H3 shRNA produced the highest knockdown effect (49% of control). Simultaneously, the empty vector or scramble shRNA was also used to establish cell lines for comparison. ER luminal free calcium measurement and survival assay on the cell lines were performed similar to the protocol used in primary neuronal cultures as described below and in the Supporting Information.

ER Luminal Free Calcium Measurements

The data acquisitions were performed with a ratiometric calcium-imaging system, which is composed of a high-speed monochromator (DeltaRAM from Photon Technology International [PTI]), an EMCCD camera (Andor), and an inverted microscope (Nikon Eclipse Ti). ER free calcium concentration ([Ca2+]ER) was determined as described previously, with minor modification (Solovyova and Verkhratsky, 2002; Solovyova et al., 2002). Briefly, SH-SY5Y cultures were loaded with mag-fura-2/AM (5 μM) and pluronic F-127 (0.05%) at 37°C for 45 min in loading buffer (125 mM NaCl, 5 mM KCl, 1 mM MgSO4, 1 mM Na2HPO4, 5.5 mM glucose, 20 mM NaHCO3, 2 mM L-glutamine, and 20 mM HEPES, pH 7.2) and then cultured in dye-free loading buffer for 45 min. These preloaded cultures were treated with 5 μM digitonin for 30–45 sec to allow dye in the cytoplasm to leak out of the cells; the culture dishes were then washed to remove residual digitonin and leaked dye. Cellular fluorescence decreased and the 340:380 ratios increased

immediately. Once the ratios had reached plateau levels and remained stable, the ratios were used to indicate ER calcium ratios as described in previous reports (Chen et al., 2004; Solovyova and Verkhratsky, 2002).

Establishment of a Rat PD Model With 6-OHDA Injections

The procedures used in our experiment repeated a previous protocol (Bjorklund et al., 1997; Cicchetti et al., 2002), with minor modifications. Briefly, unilateral (right hemisphere) intrastriatal 6-hydroxydopamine (6-OHDA) lesions were performed in rats (~250 g) under chloral hydrate anesthesia by stereotaxic injection of 6-OHDA. Eight microliters of 6-OHDA (5 μg/μl, dissolved in ascorbate/0.9 NaCl) was injected into the striatum (AP +0.7, LAT −3.5, DV −5.0 mm) at a rate of 0.5 μl/min as described (Sauer and Oertel, 1994). The needle was allowed to remain in the brain for 5 min before being retracted at the end of the 6-OHDA infusion. One month after 6-OHDA infusion, the cortex, striatum-putamen, and midbrain from intact or lesion sides were collected for immunoblotting or immunohistochemistry.

Immunohistochemistry

The 6-OHDA-lesioned rats were perfused transcardially with 4% paraformaldehyde in saline, and the brains were removed, dehydrated through graded ethanol steps and xylene, and then embedded in paraffin. Sections were cut with a vibrotome (Leica RM 2135) at a thickness of 5 μm and mounted onto glass slides. The mounted sections were, deparaffinized with xylene, and then rehydrated with graded ethanol steps from 100% to 70%. For detection of tyrosine hydroxylase (TH), the slides were incubated 1 hr with a mouse monoclonal antibody at a dilution of 1:500. The sections were subsequently washed with PBS and then incubated with biotinylated secondary antibody (1:2,000) for 30 min, followed by another set of washes and incubation with avidin-horseradish peroxidase complex for 30 min. Peroxidase activity was visualized using AEC as a red chromogen, after which the sections were counterstained with hematoxylin and mounted with neutral balsam. For CRT or ERp57 stainings, the slides were incubated with CRT antibody (1:250) or ERp57 antibody (1:10) and the peroxidase activity was visualized with AEC as a chromogen. All procedures were performed at room temperature. Observations were made under phase-contrast and brightfield microscopy (Olympus BX 41).

Proteasome Activity Assay for Neuronal Cultures and Brain Tissues

The neurons cultured in six-well plates were scraped into lysis buffer (10 mM Tris-HCl, pH 7.5, 1 mM EDTA, 2 mM ATP, 20% glycerol, 4 mM DTT), sonicated, and then centrifuged at 13,000g at 4°C for 10 min. The supernatants (2.5 μg protein) were incubated with proteasome-activity assay buffer (50 mM Tris-HCl, pH 8, 0.5 mM EDTA, 40 μm N-succinyl-Leu-Leu-Val-Tyr-7-amido-4-methylcoumain [Suc-LLVY-AMC]) for 1 hr at 37°C. The reactions were stopped by adding 0.25 ml cold water and placing the reaction mixtures on ice for at least 10 min. The intensity of fluorescence of each solution was measured by fluorescence spectrophotometry (Spectra M5; Molecular Devices) at 380 nm excitation (Ex) and 440 nm emission (Em) wavelengths, as described previously (Tsukahara et al., 1988; Qiu et al., 2000). The ratios between raw fluorescence and protein contents were used to

represent proteasome activity as described by Keller et al. (2000a). For proteasome activity assay with brain tissues, we followed the previous procedure (Keller et al., 2000a).

Statistical Analysis

The significance in each experiment was tested by one-way ANOVA and Bonferroni post hoc test if not mentioned, or otherwise by Student's t-test. Differences were considered statistically significant at $P \leq 0.05$.

RESULTS

Proteasome inhibition Decreases CRT and ERp57 Protein Levels From Whole-Cell Lysates or ER Fractions From Primary Cortical Neurons

As a first step toward studying interactions between the UPS and the ER in neurons, we determined conditions under which proteasome activity could be reproducibly inhibited without causing neurotoxicity. At 1 μM, both MG and LA consistently decreased neuronal proteasome activity significantly (~ 42% to ~ 70% of control; Supp. Info. Fig. 1) and without compromising neuronal survival (Supp. Info. Figs. 2, 3). Next, we examined the effect of proteasome inhibition on the components of CRT/CNX glycoprotein quality-control system, i.e., CRT, CNX, and ERp57; GRP78/Bip was used as a comparison. We applied MG or LA (100 nM-1 μM) to primary neuronal cultures. MG decreased CRT protein levels at 1 μM consistently in primary cortical neurons; this effect was apparent after 12 hr of treatment (~65% of control; Fig. 1A1,2), but the decrease at 24 hr was more pronounced (~50% of control; not shown). Likewise, LA at 1 μM decreased CRT at 12 hr (~50% of control; Fig. 1B1,2) and 24 hr (~45% of control; not shown) of treatment. Similar reductions in CRT protein levels were also obtained in SN neuronal cultures treated with MG/LA (data not shown). Compared with their effects on CRT, MG or LA caused diminution of ERp57 more potently. Specifically, both drugs reduced the levels ERp57 at doses as low as 0.3 μM (~70% and ~73% of control for MG and LA, respectively; Fig. 1). In contrast to the effects on CRT and ERp57, MG or LA did not change protein levels of GRP78/Bip or calnexin (Fig. 1A1,B1). A few reports have indicated that CRT and ERp57 can localize in subcellular compartments beyond the ER per se; therefore, we tested for CRT or ERp57 protein changes in ER fractions isolated from cortical neurons that had been treated with MG or LA. Because the protein yield from microsomes is scarce, we used dot blots instead of Western blots to quantify the CRT or ERp57 protein. Calnexin was not changed by MG or LA (Fig. 2A), so it was used for normalization purposes. CRT was reduced by MG in 12- and 24-hr treatments (~52% and 82% of control, normalized to calnexin; Fig. 2B,C); LA had a similar effect (~65% of control; $P < 0.05$; not shown). Likewise, ERp57 was reduced by 12- and 24-hr treatments with MG (~75% and 80% of control; Fig. 2B,C) or a 12-hr treatment with LA (~70% of control; $P < 0.05$, not shown). These findings are consistent with the Western blot results from whole-cell lysates.

Proteasome Inhibition Increases Extracellular Secretion of CRT

As described above, CRT or ERp57 protein levels in ER fractions were diminished after proteasome inhibition in neurons. There are several possible explanations for this result, one of which is that CRT or ERp57 was secreted extracellularly; another is that MG and LA, by

decreasing ER calcium, could act as ER stressors and inhibit protein synthesis generally. We tested the first hypothesis with a sandwich ELISA of culture media. Interestingly, media from cultures treated with proteasome inhibitors contained significantly higher amounts of CRT than untreated cultures (~2- to 3.75-fold of control; Fig. 3A). This effect was completely blocked by coapplication of brefeldin A, an inhibitor of protein trafficking (Fig. 3B). The normalization of CRT levels by brefeldin A (Fig. 3B) suggests that the elevation of CRT in the media after treatment with MG or LA resulted from increased transport of CRT out of the ER compartment. It is unlikely that the increased level of CRT in the media was a result of cell lysis, because there was no decrease in cell viability under these conditions (Supp. Info. Figs. 2, 3). We did not detect any change of calnexin or GRP78 induced by MG or LA in our regimens (Fig. 1), so it appears that the reduction of cellular CRT or ERp57 levels does not result from a general suppression of ER protein synthesis by MG or LA. However, we did not detect ERp57 in aliquots of concentrated supernatants with ELISA or immunoblotting, but this may be because immunodetectable levels of ERp57 are limited, at least with existing antibodies (e.g., Fig. 2).

Knockdown of CRT Increases Toxicity Toward 6-OHDA but Does Not Change ER Free Calcium Concentrations

After demonstrating that proteasome inhibition resulted in reductions in CRT or ERp57 levels, we next planned to examine the impact of reductions of these proteins on cell survival and ER luminal free calcium concentrations. Because expression of CRT is much more abundant than that of ERp57, we tested the effects of knocking down CRT. To achieve the penetrance necessary for assaying large populations of cells, we stably transfected a neuronal cell line with an shRNA construct targeted against CRT. SH-SY5Y cells were transfected with a combination of CRT-specific shRNAs, or with a vector expressing RNA of a scrambled sequence, or with empty vector; stable transfectants of each group were selected and maintained for experiments. A combination of the CRT-specific shRNAs H1 and H3, but not scrambled shRNA, decreased CRT protein levels significantly (49% of control; Fig. 4B). Tests of specificity included immunoblotting of GRP78, which was unaltered in any of the transfected lines (Fig. 4B). The established cell lines were subjected to 6-OHDA (10, 30 μM) treatment for 24 hr. CRT shRNA cells were more vulnerable (viability 41–43% of control) than those stably transfected with empty vector or scrambled RNA (viability 65–79% of control; Fig. 4C). However, knockdown of CRT in SH-SY5Y did not change ER luminal free calcium levels (Fig. 4D).

CRT and ERp57 Protein Level Are Reduced in Midbrain of PD Model Rats

Proteasome inhibition in CNS has been postulated to play a role in neuronal degeneration in Alzheimer's disease (Keller et al., 2000a), PD (McNaught et al., 2003), and other neurodegenerative disorders. One report has indicated that levels of CRT are reduced in AD brain (Taguchi et al., 2000), suggesting that there may be some association between proteasome inhibition and the CRT/CNX glycoprotein quality-control system. To test this hypothesis, we examined it in a rodent model of PD created with ventrolateral caudate-putamen (CPu) injection of 6-OHDA (Bjorklund et al., 1997; Cicchetti et al., 2002). The ipsilateral nigra showed substantial diminution of tyrosine hyroxylase (TH) staining compared with the contralateral nigra (Fig. 5A–C); the treatment produced similar effects in

CPu (not shown). We examined the proteasome activity in different brain regions. As shown in Figure 5D, proteasome activity was reduced significantly in ipsilateral nigra compared with contralateral nigra; however, the reductions were absent in the CPU or cerebral cortex from 6-OHDA-injected hemispheres compared with those from the contralateral counterparts (not shown). Furthermore, we examined the protein levels of CRT, CNX, ERp57, and GRP78/BiP in these brain regions. As shown in Figure 5E, CRT and ERp57 protein levels were reduced in 6-OHDA-lesioned midbrain homogenates (~65% and 66% of saline-injection counterpart) but not in cerebral cortex or CPu; in contrast, CNX and GRP78/BiP protein levels remained consistent between control and 6-OHDA-lesioned striatum and midbrain. To exclude the possibility that reduced CRT and ERp57 from midbrain homogenate resulted from decreased cell density fgrom 6-OHDA damage, immunostainings against CRT or ERp57 from midbrain were performed. As shown in the images in the top row of Figure 6, decreased CRT staining was found in individual intact cells (judged from morphology) from the 6-OHDA lesion side (arrowhead) compared with those from sham-treated side (arrowhead). A similar staining pattern was seen for ERp57 (Bottom row in Fig 6).

DISCUSSION

To our knowledge, this is the first systemic report to probe whether and how proteasome inhibition affects the CRT/CNX native-glycoprotein checkpoint machinery. We demonstrated that proteasome inhibition decreases the intracellular protein levels of CRT and its cochaperone, ERp57, the essential components of the CRT/CNX glycoprotein folding system. We also showed that the reductions induced by proteasome inhibition were specific for CRT and ERp57, with no change in levels of CNX or the other chaperone, GRP78. These reductions were independent of transcriptional regulation; coapplication of actinomycin D had no effect on the changes (not shown). We further indicated that proteasome inhibition increased CRT in the extracellular media, a phenomenon attenuated by a protein-trafficking inhibitor, suggesting that the reduction in CRT could be caused in part by an increase in secretion. Then, we demonstrated a negative impact on neuronal survival by knocking down the intracellular CRT. These in vitro data demonstrate a connection between proteasome inhibition and components of the CRT/CNX glycoprotein folding system, with consequences on cellular survival. We further demonstrated in vivo that CRT and ERp57 protein levels were reduced in the affected brain tissues in the 6-OHDA-lesioned rat model of PD, which contained dampened proteasome activity. Altogether, these in vivo and in vitro data suggest that proteasome inhibition, a contributing factor in neuronal death in neurodegenerative disease, may attenuate neuronal integrity via influences on the CRT/CNX glycoprotein folding system.

It is well known that proteasome inhibitors induce a wide range of cellular changes, including imbalanced oxidative status (Keller et al., 2000b; Lee et al., 2005b), calcium dyshomeostasis (Lee et al., 2005a; Wu et al., 2009), protein aggregation (Wyttenbach et al., 2000; Berke and Paulson, 2003), and regulation of transcription factor activity (Pye et al., 2003; Cai et al., 2012). To avoid nonspecific effects resulting from larger doses, we used the doses at a maximum of 1 1μM, which is at least about ten-fold lower than the doses applied in previous studies (Bush et al., 1997; Lee et al., 2005a). The treatment strengths and

durations of proteasome inhibitors used here did not compromise neuronal survival (Supp. Info. Fig. 2), and no signs of apoptosis were detected by TUNEL assay (Supp. Info. Fig. 3). However, the doses of MG/LA used here were strong enough to repress proteasome activity (Supp. Info. Fig. 1), which suggests that they have induced the expected drug effects.

Previous studies indicated that manipulations that reduce ER calcium levels also induce CRT to be secreted to the extracellular milieu or transported to the cell membrane (Tufi et al., 2008; Peters and Raghavan, 2011). We demonstrated that proteasome inhibition exerted the same effect on CRT. Although the underlying mechanisms are currently unclear, the apparent release of CRT was inhibited by brefeldin A, lending support to the conclusion that this was a controlled release rather than a reflection of cell lysis. Previously, we found that MG or LA treatments reduce ER luminal free calcium concentration in primary mouse neuronal cultures (Wu et al., 2009), and the reductions were replicated in primary rat neuronal cultures (Supp. Info. Fig. S4). These studies may shed light on the underlying mechanism by which proteasome inhibitors reduce protein levels of CRT and ERp57 and increase secretion of CRT, the processes possibly involve reduction of ER luminal calcium concentrations. CRT modulates the ER calcium pool, as reported by Bastianutto et al. (1995), so it is rational to infer that these two phenomena may have some relationship; e.g., reduction of CRT could contribute to reduced ER calcium following proteasome inhibition. However, knockdown of CRT in SH-SY5Y did not change ER luminal free calcium levels (Fig. 4D), which coincides with previous observations (Nakamura et al., 2001). Thus, if the two events are linked, it may be in the opposite direction: depressions of ER luminal calcium levels may cause the removal of CRT; this and other hypotheses are under investigation.

We found that CRT and ERp57 were reduced in the midbrain of a 6-OHDA-lesioned PD animal model. Not only were CRT and ERp57 levels reduced in protein homogenates of 6-OHDA-lesioned midbrains (Fig. 5) but immunostainings for CRT and ERp57 wered diminished in intact cells of the lesioned side (Fig. 6). These data indicate reductions in CRT and ERp57 on a cell-by-cell basis, excluding the projection that reduced CRT or ERp57 in Western blots is completely due to cytotoxicity after 6-OHDA lesion; the results suggest that the reductions of CRT and ERp57 are due to both fewer cells and lower expression in the surviving cells. Itself a chaperone protein, α-synuclein aggregates in the characteristic lesions of PD. Indeed, like CRT, α-synuclein finds its way to the extracellular space in PD and related neurodegenerative diseases (Lee et al., 2014). It is tempting to speculate that a generalized deficiency in the protein folding quality-control mechanisms, perhaps those involving the CRT/CNX checkpoint system, are seminal events in the pathology of dopaminergic circuits.

In summary, we find that proteasome inhibitors reduce intracellular protein levels of CRT and ERp57 and increase the release of CRT into the media. Experimental reduction of CRT by a shRNA strategy made neuronal cells more vulnerable to the toxicity of 6-OHDA. CRT released into extracellular compartment may leave cells deficient in an important cytoprotective mechanism, i.e., the ER glycoprotein quality-control system. These findings have implications for neuronal injury in a variety of neurodegenerative diseases linked to dysfunctions of the UPS.

Acknowledgments

We thank that our colleague, Prof. Chen Jie-Guang, for the use direction on stereotaxic facilities. The authors have no competing interests to declare.

References

Bastianutto C, Clementi E, Codazzi F, Podini P, De Giorgi F, Rizzuto R, Meldolesi J, Pozzan T. Overexpression of calreticulin increases the Ca2+ capacity of rapidly exchanging Ca2+ stores and reveals aspects of their lumenal microenvironment and function. J Cell Biol. 1995; 130:847–855. [PubMed: 7642702]

Berke SJ, Paulson HL. Protein aggregation and the ubiquitin proteasome pathway: gaining the UPPer hand on neurodegeneration. Curr Opin Genet Dev. 2003; 13:253–261. [PubMed: 12787787]

Bjorklund A, Rosenblad C, Winkler C, Kirik D. Studies on neuroprotective and regenerative effects of GDNF in a partial lesion model of Parkinson's disease. Neurobiol Dis. 1997; 4:186–200. [PubMed: 9361295]

Bukau B, Weissman J, Horwich A. Molecular chaperones and protein quality control. Cell. 2006; 125:443–451. [PubMed: 16678092]

Burns K, Duggan B, Atkinson EA, Famulski KS, Nemer M, Bleackley RC, Michalak M. Modulation of gene expression by calreticulin binding to the glucocorticoid receptor. Nature. 1994; 367:476–480. [PubMed: 8107808]

Bush KT, Goldberg AL, Nigam SK. Proteasome inhibition leads to a heat-shock response, induction of endoplasmic reticulum chaperones, and thermotolerance. J Biol Chem. 1997; 272:9086–9092. [PubMed: 9083035]

Cai J, Sun L, Lin B, Wu M, Qu J, Snider BJ, Wu S. Pretreatment with proteasome inhibitors protects against oxidative injuries via PPARalpha-dependent and -independent pathways in ARPE-19 cells. Invest Ophthalmol Vis Sci. 2012; 53:5967–5974. [PubMed: 22879419]

Chen R, Valencia I, Zhong F, McColl KS, Roderick HL, Bootman MD, Berridge MJ, Conway SJ, Holmes AB, Mignery GA, Velez P, Distelhorst CW. Bcl-2 functionally interacts with inositol 1,4,5-trisphosphate receptors to regulate calcium release from the ER in response to inositol 1,4,5-trisphosphate. J Cell Biol. 2004; 166:193–203. [PubMed: 15263017]

Cicchetti F, Brownell AL, Williams K, Chen YI, Livni E, Isacson O. Neuroinflammation of the nigrostriatal pathway during progressive 6-OHDA dopamine degeneration in rats monitored by immunohistochemistry and PET imaging. Eur J Neurosci. 2002; 15:991–998. [PubMed: 11918659]

Deng HX, Chen W, Hong ST, Boycott KM, Gorrie GH, Siddique N, Yang Y, Fecto F, Shi Y, Zhai H, Jiang H, Hirano M, Rampersaud E, Jansen GH, Donkervoort S, Bigio EH, Brooks BR, Ajroud K, Sufit RL, Haines JL, Mugnaini E, Pericak-Vance MA, Siddique T. Mutations in UBQLN2 cause dominant X-linked juvenile and adult-onset ALS and ALS/dementia. Nature. 2011; 477:211–215. [PubMed: 21857683]

Denzel A, Molinari M, Trigueros C, Martin JE, Velmurgan S, Brown S, Stamp G, Owen MJ. Early postnatal death and motor disorders in mice congenitally deficient in calnexin expression. Mol Cell Biol. 2002; 22:7398–7404. [PubMed: 12370287]

Ellgaard L, Frickel EM. Calnexin, calreticulin, and ERp57: teammates in glycoprotein folding. Cell Biochem Biophys. 2003; 39:223–247. [PubMed: 14716078]

Fadel MP, Dziak E, Lo CM, Ferrier J, Mesaeli N, Michalak M, Opas M. Calreticulin affects focal contact-dependent but not close contact-dependent cell-substratum adhesion. J Biol Chem. 1999; 274:15085–15094. [PubMed: 10329714]

Gelebart P, Opas M, Michalak M. Calreticulin, a Ca2+-binding chaperone of the endoplasmic reticulum. Int J Biochem Cell Biol. 2005; 37:260–266. [PubMed: 15474971]

Greives MR, Samra F, Pavlides SC, Blechman KM, Naylor SM, Woodrell CD, Cadacio C, Levine JP, Bancroft TA, Michalak M, Warren SM, Gold LI. Exogenous calreticulin improves diabetic wound healing. Wound Repair Regen. 2012; 20:715–730. [PubMed: 22985041]

Hochstrasser M. Ubiquitin, proteasomes, and the regulation of intracellular protein degradation. Curr Opin Cell Biol. 1995; 7:215–223. [PubMed: 7612274]

Jiang H, Fang J, Wu B, Yin G, Sun L, Qu J, Barger SW, Wu S. Overexpression of serine racemase in retina and overproduction of D-serine in eyes of streptozotocin-induced diabetic retinopathy. J Neuroinflamm. 2011; 8:119.

Jiang HY, Wek RC. Phosphorylation of the alpha-subunit of the eukaryotic initiation factor-2 (eIF2alpha) reduces protein synthesis and enhances apoptosis in response to proteasome inhibition. J Biol Chem. 2005; 280:14189–14202. [PubMed: 15684420]

Keller JN, Hanni KB, Markesbery WR. Impaired proteasome function in Alzheimer's disease. J Neurochem. 2000a; 75:436–439. [PubMed: 10854289]

Keller JN, Hanni KB, Markesbery WR. Possible involvement of proteasome inhibition in aging: implications for oxidative stress. Mech Ageing Dev. 2000b; 113:61–70. [PubMed: 10708250]

Koepp DM, Harper JW, Elledge SJ. How the cyclin became a cyclin: regulated proteolysis in the cell cycle. Cell. 1999; 97:431–434. [PubMed: 10338207]

Lee CS, Han ES, Han YS, Bang H. Differential effect of calmodulin antagonists on MG132-induced mitochondrial dysfunction and cell death in PC12 cells. Brain Res Bull. 2005a; 67:225–234. [PubMed: 16144659]

Lee CS, Han ES, Park ES, Bang H. Inhibition of MG132-induced mitochondrial dysfunction and cell death in PC12 cells by 3-morpholinosydnonimine. Brain Res. 2005b; 1036:18–26. [PubMed: 15725397]

Lee HJ, Bae EJ, Lee SJ. Extracellular alpha-synuclein—a novel and crucial factor in Lewy body diseases. Nat Rev Neurol. 2014 in press.

Li Y, Liu L, Barger SW, Mrak RE, Griffin WS. Vitamin E suppression of microglial activation is neuroprotective. J Neurosci Res. 2001; 66:163–170. [PubMed: 11592111]

McNaught KS. Proteolytic dysfunction in neurodegenerative disorders. Int Rev Neurobiol. 2004; 62:95–119. [PubMed: 15530569]

McNaught KS, Jenner P. Proteasomal function is impaired in substantia nigra in Parkinson's disease. Neurosci Lett. 2001; 297:191–194. [PubMed: 11137760]

McNaught KS, Belizaire R, Isacson O, Jenner P, Olanow CW. Altered proteasomal function in sporadic Parkinson's disease. Exp Neurol. 2003; 179:38–46. [PubMed: 12504866]

Mesaeli N, Nakamura K, Zvaritch E, Dickie P, Dziak E, Krause KH, Opas M, MacLennan DH, Michalak M. Calreticulin is essential for cardiac development. J Cell Biol. 1999; 144:857–868. [PubMed: 10085286]

Nakamura K, Zuppini A, Arnaudeau S, Lynch J, Ahsan I, Krause R, Papp S, De Smedt H, Parys JB, Muller-Esterl W, Lew DP, Krause KH, Demaurex N, Opas M, Michalak M. Functional specialization of calreticulin domains. J Cell Biol. 2001; 154:961–972. [PubMed: 11524434]

Nguyen TO, Capra JD, Sontheimer RD. Calreticulin is transcriptionally upregulated by heat shock, calcium and heavy metals. Mol Immunol. 1996; 33:379–386. [PubMed: 8676889]

Paschen W. Endoplasmic reticulum: a primary target in various acute disorders and degenerative diseases of the brain. Cell Calcium. 2003; 34:365–383. [PubMed: 12909082]

Peters LR, Raghavan M. Endoplasmic reticulum calcium depletion impacts chaperone secretion, innate immunity, and phagocytic uptake of cells. J Immunol. 2011; 187:919–931. [PubMed: 21670312]

Pye J, Ardeshirpour F, McCain A, Bellinger DA, Merricks E, Adams J, Elliott PJ, Pien C, Fischer TH, Baldwin AS Jr, Nichols TC. Proteasome inhibition ablates activation of NF-kappa B in myocardial reperfusion and reduces reperfusion injury. Am J Physiol Heart Circ Physiol. 2003; 284:H919–H926. [PubMed: 12424098]

Qiu JH, Asai A, Chi S, Saito N, Hamada H, Kirino T. Proteasome inhibitors induce cytochrome c-caspase-3-like protease-mediated apoptosis in cultured cortical neurons. J Neurosci. 2000; 20:259–265. [PubMed: 10627603]

Rauch F, Prud'homme J, Arabian A, Dedhar S, St-Arnaud R. Heart, brain, and body wall defects in mice lacking calreticulin. Exp Cell Res. 2000; 256:105–111. [PubMed: 10739657]

Sauer H, Oertel WH. Progressive degeneration of nigrostriatal dopamine neurons following intrastriatal terminal lesions with 6-hydroxydopamine: a combined retrograde tracing and immunocytochemical study in the rat. Neuroscience. 1994; 59:401–415. [PubMed: 7516500]

Solovyova N, Verkhratsky A. Monitoring of free calcium in the neuronal endoplasmic reticulum: an overview of modern approaches. J Neurosci Methods. 2002; 122:1–12. [PubMed: 12535760]

Solovyova N, Veselovsky N, Toescu EC, Verkhratsky A. Ca2+ dynamics in the lumen of the endoplasmic reticulum in sensory neurons: direct visualization of Ca2+-induced Ca2+ release triggered by physiological Ca2+ entry. EMBO J. 2002; 21:622–630. [PubMed: 11847110]

Taguchi J, Fujii A, Fujino Y, Tsujioka Y, Takahashi M, Tsuboi Y, Wada I, Yamada T. Different expression of calreticulin and immunoglobulin binding protein in Alzheimer's disease brain. Acta Neuropathol. 2000; 100:153–160. [PubMed: 10963362]

Tashiro Y, Urushitani M, Inoue H, Koike M, Uchiyama Y, Komatsu M, Tanaka K, Yamazaki M, Abe M, Misawa H, Sakimura K, Ito H, Takahashi R. Motor neuron-specific disruption of proteasomes, but not autophagy, replicates amyotrophic lateral sclerosis. J Biol Chem. 2012; 287:42984–42994. [PubMed: 23095749]

Tsukahara T, Ishiura S, Sugita H. An ATP-dependent protease and ingensin, the multicatalytic proteinase, in K562 cells. Eur J Biochem. 1988; 177:261–266. [PubMed: 3142770]

Tufi R, Panaretakis T, Bianchi K, Criollo A, Fazi B, Di Sano F, Tesniere A, Kepp O, Paterlini-Brechot P, Zitvogel L, Piacentini M, Szabadkai G, Kroemer G. Reduction of endoplasmic reticulum Ca2+ levels favors plasma membrane surface exposure of calreticulin. Cell Death Differ. 2008; 15:274–282. [PubMed: 18034188]

Waser M, Mesaeli N, Spencer C, Michalak M. Regulation of calreticulin gene expression by calcium. J Cell Biol. 1997; 138:547–557. [PubMed: 9245785]

Wu S, Hyrc KL, Moulder KL, Lin Y, Warmke T, Snider BJ. Cellular calcium deficiency plays a role in neuronal death caused by proteasome inhibitors. J Neurochem. 2009; 109:1225–1236. [PubMed: 19476541]

Wu SZ, Bodles AM, Porter MM, Griffin WS, Basile AS, Barger SW. Induction of serine racemase expression and D-serine release from microglia by amyloid beta-peptide. J Neuroinflamm. 2004; 1:2.

Wyttenbach A, Carmichael J, Swartz J, Furlong RA, Narain Y, Rankin J, Rubinsztein DC. Effects of heat shock, heat shock protein 40 (HDJ-2), and proteasome inhibition on protein aggregation in cellular models of Huntington's disease. Proc Natl Acad Sci U S A. 2000; 97:2898–2903. [PubMed: 10717003]

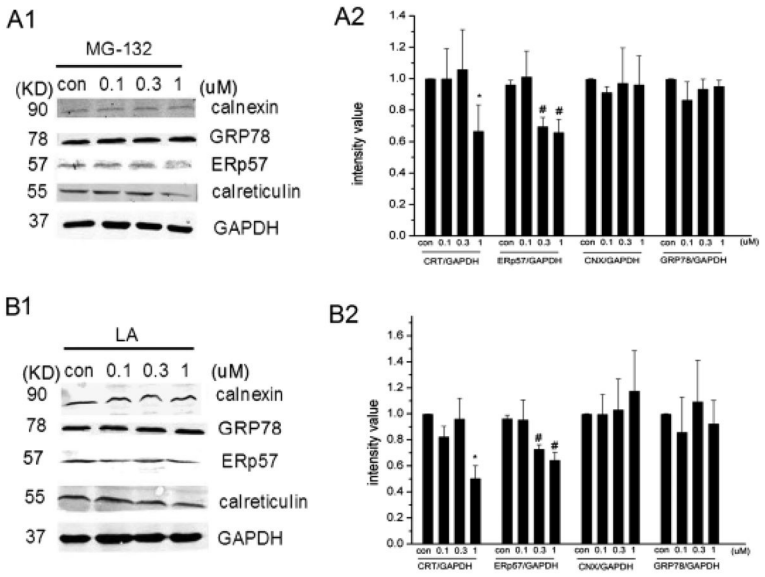

Figure 1.

Proteasome inhibitors decrease CRT or ERp57 but not CNX protein levels in cortical neurons. After 8 days in culture, rat primary cortical neurons (CX) were exposed to MG (A1) or LA (B1) for 12 hr at concentrations ranging from 100 nM to 1 μM. Lysates containing equal amounts of protein were subjected to Western blot analysis of CRT (1:250), ERp57 (1:500), CNX (1:1,000), or GRP78 (1:1,000). The ratios of CRT/GAPDH,ERp57/GAPDH, CNX/GAPDH, and GRP78/GAPDH were quantified from at least six experiments (A2,B2). The blots shown are typical of six determinations. *,#$P < 0.05$ vs. nontreatment.

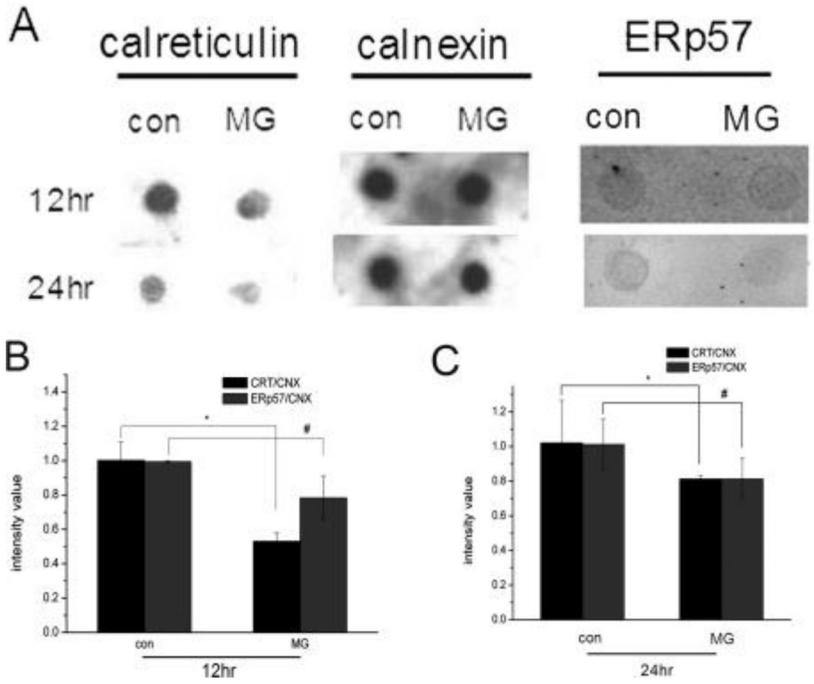

Figure 2.

Reduction of CRT or ERp57 but not CNX protein levels in ER fractions from cortical neurons treated by proteasome inhibitors. A: ER fractions were isolated from cortical cultures treated with MG (1 μM) for 12 or 24 hr, and semiquantification with dot blot was performed as described in Materials and Methods. The blots shown are typical of triplicate determinations. B,C: The results were quantified with the ratios between CRT and calnexin or ERp57 and calnexin; data represent triplicate experiments. *,#$P < 0.05$ vs. nontreatment. Comparisons between treatment and nontreatment were assessed with Student's t-test.

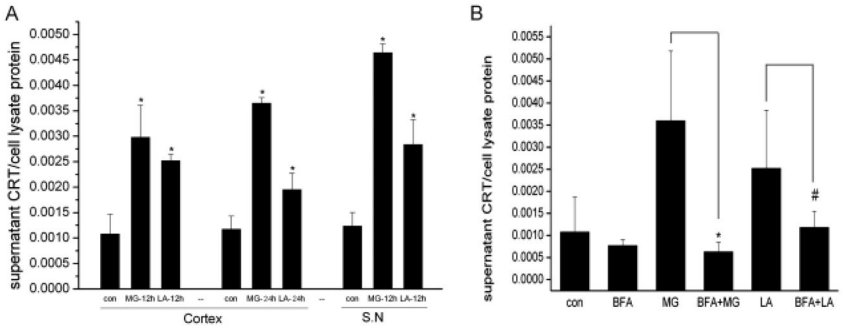

Figure 3.

Proteasome inhibitors increase CRT secretion to extracellular compartment. A: Culture media from 12-hr MG- or LA-treated cortical and SN cultures was subjected to a sandwich ELISA for detection of CRT. The values indicate levels of CRT in culture media relative to total cell lysates from at least triplicate determinations. *P < 0.05 vs. control. B: Culture media from cortical cultures treated with MG/LA for 12 hr or with a combination of brefeldin A (BFA; 100 ng/ml) were subjected to detection of CRT by ELISA. These values also indicate levels of CRT in culture media relative to total cell lysates from at least triplicate determinations. *,#P < 0.05, MG/LA-treated conditions vs. their combinations with BFA.

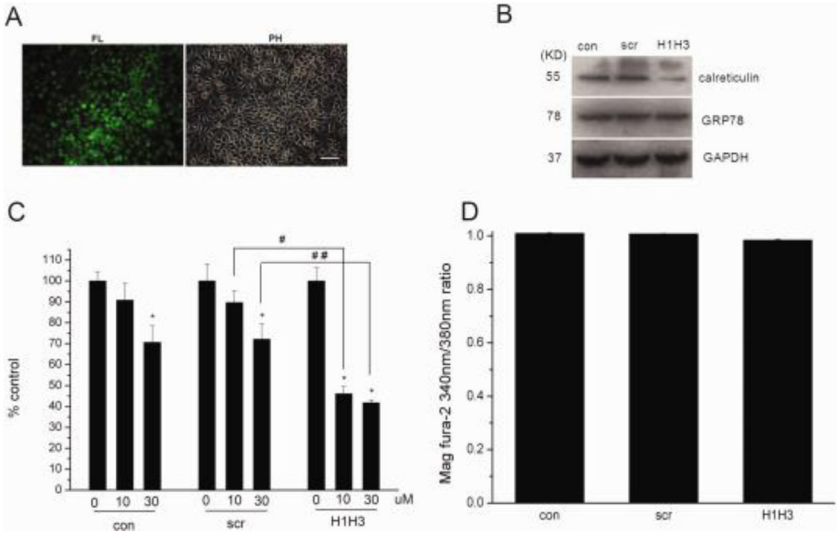

Figure 4.

CRT knockdown increases toxicity toward 6-OHDA. SH-SY5Y cells were stably transfected with empty vector (con), a vector expressing RNA of a scrambled sequence (scr), or vectors expressing CRT shRNA (H1H3). A: The vectors also express GFP, and this was dectectable in a fluorescence (FL) image of the H1H3 clone; a phase-contrast (PH) image is shown for comparison. B: Proteins were extracted from the three types of stable cell lines and immunoblotted for CRT, GRP78, and GAPDH. C: The three types of cell lines were treated with 6-OHDA (10, 30 μM) for 24 hr and subjected to MTS assay. The results shown are the average of triplicate experiments. *$P < 0.05$ vs. control; #$P < 0.05$ scr vs. H1H3, 10 μM 6-OHDA; ##$P < 0.0001$ scr vs. H1H3, 30 μM 6-OHDA. D: The three types of cell lines were subjected to ER luminal free calcium assay. The results shown are the average of triplicate experiments. Scale bar = 100 μm.

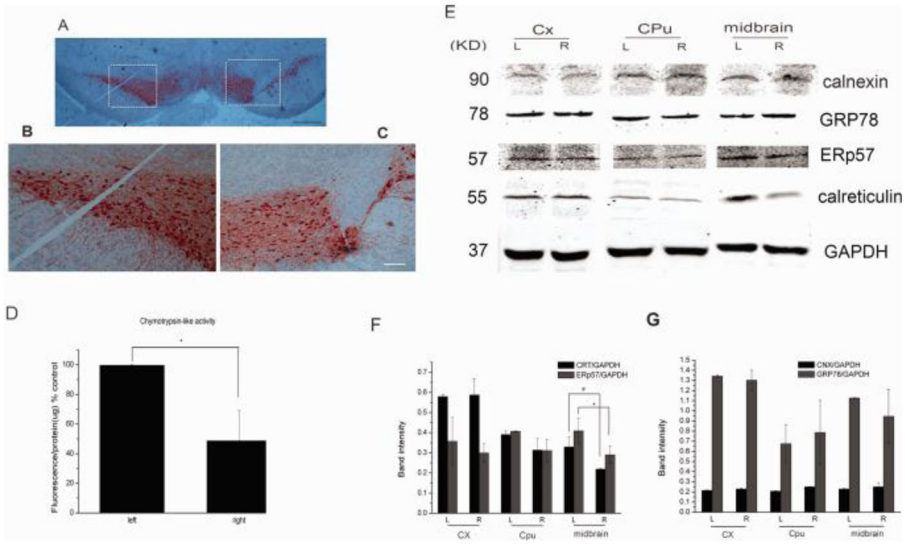

Figure 5.

Specific reduction of CRT or ERp57 in midbrain of 6-OHDA-lesioned rat. Rats were subjected to a unilateral (right side) injection of 6-OHDA, followed by a 1-month survival. A: Immunohistochemistry for tyrosine hydroxylase (TH). The boxed areas are enlarged in B,C. Fewer dopaminergic neurons in SN are present in the 6-OHDA-lesioned ipsilateral side (right, B) than in the contralateral side (left, C). D: Tissues from the midbrains of ipsilateral (R) and the contralateral sides of 6-OHDA-lesioned rats (L) were subjected to proteasome activity assay as described in Materials and Methods. The results are expressed as the ratios between fluorescence values and protein content; the values from nonlesioned midbrains were set as 100%, and the values from the lesioned sides were normalized accordingly. The results shown are mean (±SEM) from five rats (*$P < 0.05$). E: Homogenates from cerebral cortex (Cx), striatum-putamen (CPu), and midbrain from ipsilateral (R) and contralateral (L) sides of 6-OHDA-lesioned rat were subjected to immunoblotting with GRP78, CRT, ERp57, and CNX; GAPDH served as an internal control. The results shown are typical of eight rats. The results were quantified as the ratios of CRT/GAPDH, ERp57/GAPDH (F; *,#$P < 0.05$ R vs. L) or GRP78/GAPDH, or CNX/GAPDH (G) averaged from eight rats. Scale bars = 20 μm in A; 50 μm in B,C.

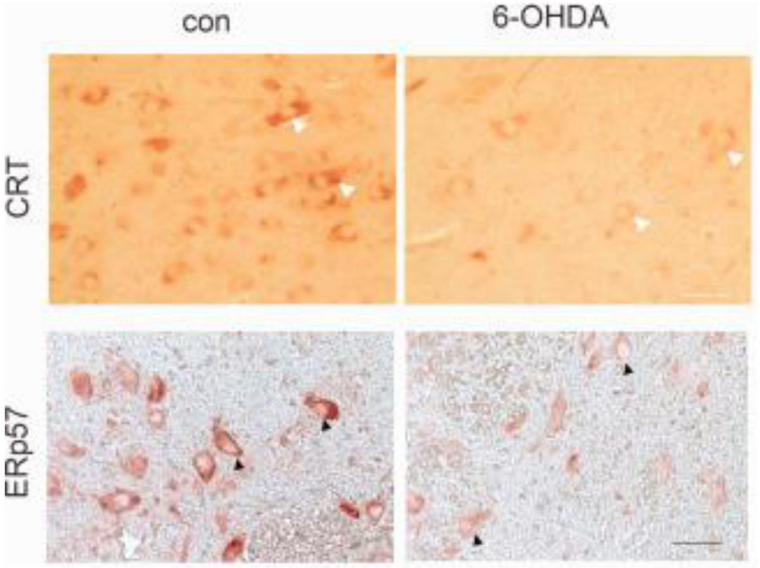

Figure 6.

Reductions of CRT and ERp57 staining in midbrain of 6-OHDA-lesioned rats. Midbrains from ipsilateral and contralateral sides of 6-OHDA-lesioned rat were subjected to immunohistochemistry with CRT (top row, white arrowheads) or ERp57 (bottom row, black arrowheads). The stainings for cerebral cortex (Cx) and striatum-putamen (CPu) did not show differences for nonlesioned and lesioned sides and thus are not shown here. The images are representative of triplicate experiments from five rats. Scale bars = 20 μm.